Science of the Total Environment 926 (2024) 171858

Contents lists available at ScienceDirect

Science of the Total Environment

journal homepage: www.elsevier.com/locate/scitotenv

Mediterranean pine forest decline: A matter of root-associated microbiota and climate change

Ana V. Lasa [a], Antonio José Fernández-González [a], Pablo J. Villadas [a], Jesús Mercado-Blanco [a], Antonio J. Pérez-Luque [b,c], Manuel Fernández-López [a,*]

[a] Department of Soil and Plant Microbiology, Estación Experimental del Zaidín, CSIC, Profesor Albareda 1, 18008 Granada, Spain
[b] Department of Assesment, Restoration and Protection of Mediterranean Agrosystem (SERPAM), Estación Experimental del Zaidín, CSIC, Profesor Albareda 1, 18008 Granada, Spain
[c] Institute of Forest Sciences ICIFOR, INIA-CSIC. Ctra. La Coruña km 7.5, 28040, Madrid, Spain

HIGHLIGHTS

- Mediterranean *Pinus sylvestris* forests are severely affected by decline phenomenon.
- The role of root and soil microbiota on pine forests decline is unknown.
- Metabarcoding was used to compare root microbiota of affected and unaffected pines.
- Microbial communities were different for both trees subjected to the same climate.
- Affected trees were more enriched in the phytophatogen '*Ca.* Phytoplasma pini'.

GRAPHICAL ABSTRACT

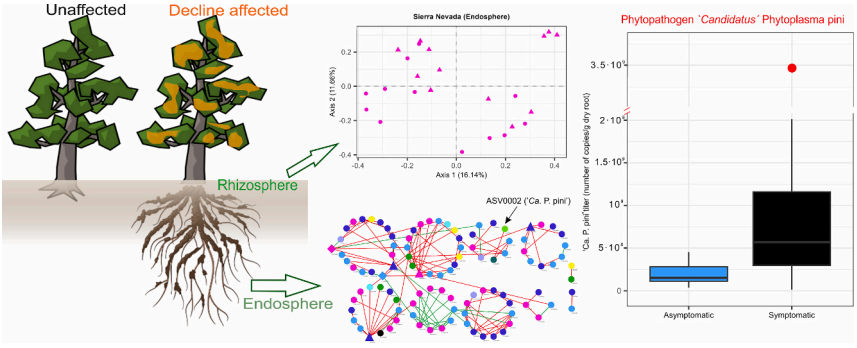

ARTICLE INFO

Editor: Charlotte Poschenrieder

Keywords:
Pine forest decay
Rhizosphere microbiota
Root endosphere microbiota
Phytoplasmas
Pathogen detection
Sierra Nevada National Park

ABSTRACT

Forest ecosystems worldwide currently face worrying episodes of forest decline, which have boosted weakening and mortality of the trees. In the Mediterranean region, especially in the southeast Iberian Peninsula, *Pinus sylvestris* forests are severely affected by this phenomenon, and it has been commonly attributed to drought events. Remarkably, the role of root microbiota on pine decline has been overlooked and remains unclear. We therefore used metabarcoding to identify the belowground microbial communities of decline-affected and unaffected pine trees. Taxonomic composition of bacterial and fungal rhizosphere communities, and fungal populations dwelling in root endosphere showed different profiles depending on the health status of the trees. The root endosphere of asymptomatic trees was as strongly dominated by '*Candidatus* Phytoplasma pini' as the root of decline-affected pines, accounting for >99 % of the total bacterial sequences in some samples. Notwithstanding, the titer of this phytopathogen was four-fold higher in symptomatic trees than in symptomless ones. Furthermore, the microbiota inhabiting the root endosphere of decline-affected trees assembled into a less complex and more modularized network. Thus, the observed changes in the microbial communities could be a cause or a

* Correspondence to: M. Fernández-López, Department of Soil and Plant Microbiology, Estación Experimental del Zaidín, CSIC, Profesor Albareda 1, 18008 Granada, Spain.
E-mail addresses: ana.vicente@eez.csic.es (A.V. Lasa), antonio.fernandez@eez.csic.es (A.J. Fernández-González), pablo.villadas@eez.csic.es (P.J. Villadas), jesus.mercado@eez.csic.es (J. Mercado-Blanco), manuel.fernandez@eez.csic.es (M. Fernández-López).

https://doi.org/10.1016/j.scitotenv.2024.171858
Received 10 January 2024; Received in revised form 19 March 2024; Accepted 19 March 2024
Available online 22 March 2024

consequence of forest decline phenomenon. Moreover, '*Ca*. Phytoplasma pini' is positively correlated to *Pinus sylvestris* decline events, either as the primary cause of pine decline or as an opportunistic pathogen exacerbating the process once the tree has been weaken by other factors.

1. Introduction

Forest decline is a complex phenomenon characterized by a generalized deterioration of forest stands (reduced growth, yellowing, defoliation) that can even culminate in the death of the trees. Decline episodes have been detected worldwide (Allen et al., 2010), being the Mediterranean basin a hotspot of this phenomenon due to increasing temperatures and intense and frequent droughts (Ali et al., 2022). One of the species undergoing a severe and accelerated decline process is the Scots pine (*Pinus sylvestris* L.), for which a drastic reduction (nearly 90 %) of its habitat in the Iberian Peninsula has been predicted by the end of the 21st century (Martínez-Vilalta et al., 2012). In 2017, 314.8 ha of the National Park of Sierra Nevada (Granada and Almeria provinces, Southerneast Spain) forested with this species were affected by pine decline (Authorities of the National Park of Sierra Nevada, personal communication).

Forest decline is thought to be driven by a multiplicity of biotic and abiotic factors interacting with each other (Allen et al., 2010). Indeed, it has commonly considered the following conceptual model to better understand the decline process: at the starting point, "predisposing factors" (i.e. high stand density) expose trees to long-term stresses thereby increasing their susceptibility to severe short-term stresses called "inciting factors" (i.e. droughts, infection by non-lethal pathogens). Thereafter, the so-called "contributing factors" (e.g. lethal-pathogens or pests) eventually produce tree mortality (Manion, 1991). Some authors have already proposed a positive correlation between pine decline events and severe drought periods in the Iberian Peninsula (Carnicer et al., 2011; Sánchez-Salguero et al., 2012; Vidal-Macua et al., 2017). However, the idea that forest decline is caused by multiple factors is gaining momentum (Calvão et al., 2019; Connor et al., 2021).

For a better understanding of decline episodes, pine trees should not be considered as standalone entities, but as holobionts: plant hosts and their associated microbiota. In particular, root microorganisms deploy essential functions that affect positively tree hosts, for example, by providing essential nutrients from the soil and/or protection their host from biotic and abiotic stresses (Uroz et al., 2016). In woody plants, alterations of microbial communities or imbalances can entail a disruption of the essential functions needed to keep the holobiont fitness, which could be related to decline events (Bettenfeld et al., 2020). For instance, Guo et al. (2020) reported that the infection of *Pinus massoniana* individuals by the pinewood nematode (*Bursaphelenchus xylophilus)* triggered shifts in the bacterial population inhabiting the rhizosphere soil of the host. Alterations of the diversity and structure of the root microbiota of *Pinus radiata* have also been observed when host trees are subjected to nitrogen fertilization (Gallart et al., 2018).

The contribution of microbial communities and phytopathogens to forest decline remains almost unknown, and most of the works have focused on acute oak decline (Denman et al., 2018) or on the pine wood nematode (*Bursaphelenchus xylophilus*; Proença et al., 2017). In coniferous hosts, infections with phytoplasmas (insect-borne bacterial obligate parasites) entail defoliation, dwarfed needles, yellowing, stunted growth or uncrontrolled shoot branching than can result in ball-like structures known as "witches' broom" (Marcone et al., 2021). These phloem-resident pathogens can have strong impact on the fitness of host plant. In some species, the host tree can even succumb to the pathogen, causing devastating ecological and economic losses worldwide (Stone and Putnam, 2004; Trujillo-Toro and Navarro-Cerrillo, 2019). '*Candidatus* Phytoplasma pini' has already been identified in several conifers in different European countries, including Spain (Schneider et al., 2005; Śliwa et al., 2008; Kamińska et al., 2011; Valiunas et al., 2015; Trujillo-Toro and Navarro-Cerrillo, 2019). However, its distribution in *Pinus sylvestris* stands has been poorly addressed. Infections by '*Candidatus* Phytoplasma pini' and other biotic and abiotic stressors share the same symptomatology. Therefore, deciphering the weight of each factor in the decline process is a grueling task.

Thus, in this work we aimed at uncovering the diversity, richness, taxonomic composition and associative patterns of bacterial and fungal communities dwelling in the rhizosphere and root endosphere of Scots pine trees. In particular, we selected three geographic units in southeast Spain (Autonomous region of Andalusia) where asymptomatic and/or decline-affected Scots pines were found. Moreover, we investigated the presence of '*Candidatus* Phytoplasma pini' in *Pinus sylvestris* trees either presenting evident symptoms of pine decline or being symptomless. Eventually, we analyzed the temperatures and rainfall patterns of the three selected locations. We tested the following hypotheses; 1) the root microbial communities of decline-affected pines are different compared to populations present in asymptomatic pines; 2) '*Candidatus* Phytoplasma pini' is spread among pine forests under study that show symptoms of pine decline; and 3) drought alone is not the triggering factor for pine decline in the mountainous areas under study.

2. Material and methods

2.1. Experimental area

Sampling was carried out in three mountainous protected areas in Andalusia (southeast Spain). Firstly, Sierra de Almijara was selected, where no pine trees affected by decline were detected (ASH samples, asymptomatic). Secondly, both asymptomatic and decline affected pines (NSH and NSD, respectively) were selected in the National Park of Sierra Nevada. Finally, the Natural Park of Sierra de Baza was chosen since it is so drastically affected by pine decline that only affected trees were identified (BSD samples). The specific coordinates and characteristics of each forest stand are summarized in Table S1. Pine trees were visually classified as decline-affected (symptomatic) if they showed yellowing of the crown, stunted growth and defoliation. No symptoms of common microbial diseases or pests were observed.

2.2. Obtaining of climatic data

To characterize the climatic conditions at each sampling site, we utilized high-resolution climatic maps (spatial resolution of 500 m) sourced from the Andalusian Information Subsystem for Environmental Climatology (Andalusian Environmental Information Network, https://www.juntadeandalucia.es/medioambiente/servtc5/WebClima/). These maps encompassed monthly averages of mean, minimum, and maximum temperatures, in addition to annual cumulative rainfall data. Maps were constructed by integrating data from over 200 meteorological stations. For each individual sampling site, we extracted temporal data series spanning from 1980, covering each of the climatic variables. Subsequently, we computed the yearly average values for these variables.

Drought conditions of the sites were characterized using the SPEI (Standardized Precipitation-Evapotranspiration Index) (Vicente-Serrano et al., 2010) (SPEI 6-month scale). Data were downloaded from the Spanish Drought Monitoring System (https://monitordesequia.csic.es/monitor; Vicente-Serrano et al., 2022). To compare differences of drought conditions among sites, we performed Pearson correlation among temporal series (since year 2000) with bootstraped confidence intervals. We also identified severe drought events occurring at each site

since the year 2000. A severe drought event starts when SPEI falls below the threshold of −1.28 (Páscoa et al., 2017; Spinoni et al., 2017). A drought event is considered only when SPEI values fall below that threshold for at least two consecutive months. For each drought event the "*duration*" (the number of consecutive months at which the SPEI was lower than a certain threshold) and the "*intensity*" (the mean value of the SPEI during the drought event) paremeters were computed.

2.3. Sample collection and processing

All samples were taken in the spring of 2022 (see Table S1) during the active vegetative growth phase of the trees. 12 trees by each site and condition ($N = 48$; ASH, 12; NSH 12, NSD 12, BSD 12) were sampled, following the experimental design plotted in Fig. S1. Rhizosphere soil samples were collected according to Lasa et al. (2022). Soil closely attached to the roots (rhizosphere soil) was collected by rubbing the roots manually. These roots were then collected and conserved at 4 °C until further processing within 24 h of sampling. For each tree, rhizosphere soil samples and roots were taken from two different points of the root system (2 × 48 trees). An additional soil sample (500 g) was collected near the collected roots of each tree, at the same moment that rhizospheres were sampled, to determine physicochemical parameters. These soil samples were analyzed by Laboratorio Analítico Bioclínico (https://www.lab-sl.com/en/; Almería, Spain) by standardized procedures, applying electrometric, ICP-MS (Inductively Coupled Plasma Mass Spectrometry), ion chromatrographic, volumetric, spectrophotometric or densimetric approaches.

For root surface sterilization, the protocol described by Fernández-González and collaborators (2020) was followed. Surface-sterilized roots were lyophilized at −45 °C for 72 h using a Thermo Savant Modulyo D-230 (Waltham, MA, United States) equipment, and subsequently ground with the help of sterilized grinding balls (20 mm diameter) at 30 Hz for 1 min by means of the grinder MM-400 (Retsch, Haan, Germany). Ground root material was inmediately processed.

2.4. DNA extraction and Illumina sequencing

Total DNA was extracted from 0.25 g of rhizosphere soil and 0.1 g of root material using the DNeasy® PowerSoil® Pro and DNeasy® Plant Pro Kits (Qiagen; Hilden, Germany), respectively, following the manufacturer's instructions. For both rhizosphere and root endosphere samples, DNA extracted from the two samples collected from the same tree was mixed into a composite sample. Hence, a total of 96 composite samples of DNA (48 from the root endosphere and 48 from the rhizosphere soil) were obtained (see Fig. S1). DNA yields were quantified using the fluorometer Qubit 3.0 (Life Technologies; Carlsbad, CA, United States).

DNA from each individual sample was sequenced through Illumina MiSeq platform, following a 2 × 275 PE strategy at the genomics service of the Institute of Parasitology and Biomedicine López-Neyra (CSIC; Granada, Spain). Rhizosphere prokaryotic libraries were prepared by amplifying the hypervariable regions V3-V4 of the gene *16S rRNA* using the primers Pro341F and Pro805R described by Takahashi et al. (2014). For endosphere prokaryotic libraries, V3-V4 amplicons were treated with PNA PCR clamps to minimize the plastids and mitochondrial DNA amplification (Lundberg et al., 2013). On the other hand, primers ITS4 (White et al., 1990) and fiTS7 (Ihrmark et al., 2012) were used to sequence the fungal ITS2 region. In each sequencing run, three samples of the mock community ZymoBIOMICS Microbial Community Standard II, logarithmic distribution (ZYMO Research; Irvine, CA, United States) were included as quality sequencing controls, as suggested by Bokulich et al. (2013).

2.5. Illumina data processing

Bioinformatic analyses of the dataset obtained by high-throughput sequencing were fully performed by using R software, version 4.2.3 (R Core Team, 2022). Processing of fungal and prokaryotic reads was carried out in the same manner, except otherwise indicated. Just in the case of the prokaryotic dataset, Figaro bioinformatic tool (Sasada et al., 2020) was used to establish the best parameters of the sequence trimming step. The trimming was carried out using the function *filterAndTrim* of package DADA2 (Callahan et al., 2016), removing reads with sequence ambiguities and trimming the remaining sequences at the positions proposed by Figaro. For both prokaryotic and fungal sequences, primers were removed by means of Cutadapt tool (Martin, 2011), and in the case of fungal libraries the filtering and trimming step was subsequently performed. For both prokaryotic and fungal reads, modelling of parametric errors and their correction was carried out (function *learnErrors* of DADA2). Forward and reverse reads were merged by using default parameters of the function *mergePairs* and an ASV (Amplicon Sequencing Variant) table was constructed. A chimera removal step was implemented (function *removeBimeraDenovo*, package DADA2). High-quality sequences were taxonomically classified using a modified version of the Ribosomal Database Project (RDP-II; Cole et al., 2014) training set v.18 and UNITE v. 7.2 database (Abarenkov et al., 2022) for prokaryotic and fungal reads, respectively (function *assignTaxonomy*). According to the detection limit stablished with the mock community, all the ASVs accounting for <0.0018 % of the total high-quality sequences of each corresponding library (prokaryotic or fungal) were removed from the analysis. Those ASVs classified as mitochondria, chloroplasts, and unclassified sequences at Kingdom level were not retained for further analyses, and ASVs identified as Eukaryota were eliminated from the prokaryotic dataset. We also compared those prokaryotic sequences classified as phylum "Cyanobacteria/Chloroplast" against those held in GenBank database by BLASTn, and removed all of them classified as eukaryotic organisms.

2.6. Ecological analyses

2.6.1. Rarefaction curves and alpha diversity

The rarefaction curves were obtained by the function *rarecurve*, package vegan; Oksanen et al., 2022). A rarefaction step was performed to the smallest library size prior to alpha indices calculation in order to minimize the biases associated with different sample sizes; for that purpose, function *rarefy_even_depth* of the package phyloseq (McMurdie and Holmes, 2013) was implemented. The number of observed ASVs, Shannon, Inverse of Simpson and Pielou's indices were obtained by means of the funcion *estimate_richness* (package phyloseq).

2.6.2. Beta diversity

Hereafter, non-rarefied data were considered for subsequent analyses, according to the suggestions made by McMurdie and Holmes (2014). Beta diversity analyses were performed as detailed in Supplementary Information. Briefly, ASV sequence counts were firstly normalized by the Trimmed Means of M-value (TMM), and all multivariate analyses were performed based on Weighted UniFrac distance and Bray-Curtis dissimilarity measure for prokaryotic and fungal datasets, respectively.

Constrained Analysis of Principal Coordinates (CAP) was carried out by building an environmental model with the all the measured edaphic properties and fitting them onto the multivariate ordination (Supplementary Information).

The differences among the microbial populations were visualized by means of a Principal Coordinate Analysis (PCoA) as detailed in Supplementary Information. It should be mentioned that multivariate statistical analyses were solely performed with the Sierra Nevada dataset, as this is the only geographical site where trees with and without symptoms of forest decline were observed. Thus, the dispersion of each group of samples was firstly calculated and then compared by applying permutational analysis of variance (PERMANOVA) test.

2.6.3. Differential abundance analysis

Differences in taxa abundance between symptomatic and asymptomatic trees were calculated by implementing the analysis of composition of microbiomes with bias correction (ANCOM-BC) developed by Lin and Peddada (2020). For that purpose, function *ancombc2* (package ANCOMBC) was run, excluding those taxa that were present in <10 % of the samples analyzed.

2.7. Co-occurrence network construction and comparison

Co-occurrence (association) networks were inferred just for rhizosphere soil and root endosphere samples obtained from Sierra Nevada (the only geographic unit where asymptomatic and symptomless pine trees were found). For that purpose, the Molecular Ecological Network Analysis Pipeline (MENAP) was employed (http://ieg4.rccc.ou.edu/mena/main.cgi), following the details included in Supplementary Information. In brief, aiming at diminishing the amount of random interactions, a prevalence filter was applied for both rhizosphere and root endosphere samples. ASVs abundances were log-transformed and a similarity matrix was constructed (Supplementary Information). Indirect interactions among microorganisms were discarded from the analyses and subsequently, module calculation was performed. Once association networks were inferred, a randomization step was carried out by calculating random networks and the main topological properties of empirical networks were statistically compared as described in Supplementary Information. Association networks were plotted by means of Cytoscape v.3.7.2 software (Shannon et al., 2003). Finally, ASVs included in each network were classified as connectors, module or network hubs and peripherals according to Olesen et al. (2017).

2.8. Cloning and sequencing of 16S rRNA gene

16S rRNA gene was amplified from root endosphere samples of one symptomatic and another symptomless tree (NSH01 and NSD01 samples, respectively) by using the 9bfm/1512Ur primer pair (Mühling et al., 2008) at a final concentration of 0.4 μM, and by using the AccuStart II PCR SuperMix (QuantaBio; Beverly, MA, United States). PCR conditions were the same as described by Lasa et al. (2019). PCR products were purified by using the Illustra MicroSpin S-300 HR columns (Cytiva; Little Chalfont, United Kingdom) according to the manufacturer's instructions. Purified PCR products were then ligated into the vector pGEM®-T Easy (Promega, United States) following the manufacturer's instructions, and plasmids were transformed into chemically competent *Escherichia coli* DH5α cells. Positive colonies were selected based on white-blue color strategy and the size of the insert was checked by PCR amplification with the SP6/T7 primer pair (Promega; Madison, Wi, United States). PCR conditions were the same as Lasa and collaborators (2019) but running 30 cycles and raising the annealing temperatute at 56 °C (30 s). Amplicons were sequenced on an ABI PRISM 3130xl Genetic Analyzer using the BigDye® Terminator Cycle Sequencing kit (Applied BioSystems; Waltham, MA, United States) at the genomics service of the Institute of Parasitology and Biomedicine López-Neyra. Reads were compared to that held in GenBank and EzBioCloud 16S rRNA databases (Yoon et al., 2014). They were aligned using the bioinformatic tool MAFFT v.7, and a phylogenetic tree was inferred by using the Maximum Likelihood method based on General Time Reversible model on Mega software version X (Kumar et al., 2018). Confidence values for nodes were calculated by bootstrap analysis performing 1000 permutations of the dataset.

2.9. Phytoplasma titer determination

Real-time quantitative PCR (qPCR) TaqMan® assay was performed to measure the titer of phytoplasma in the root endosphere of symptomatic and symptomless trees located at Sierra Nevada. The measurement was performed by modifying the protocol proposed by the European and Mediterranean Plant Protection Organization (EPPO, 2018), as described in Supplementary Information. The probe Pr-CaPpini (5'-FAM-TGACGGGATCCCGCACAAGCG-TAMRA-3') designed in this work to detect specifically '*Ca. P. pini*' was used (Table S2), and dilution series of a standard from 10^7 to 10^3 copies were made for titer determination (Supplementary Information). Values of threshold cycles (Ct) were recorded and the target gene copy number was calculated from standard curves.

2.10. Univariate statistical analyses

All the univariate statistical tests were computed in R software as detailed in Supplementary Information. The normality and homoscedasticity of the data and the presence of extreme outliers were studied. If data met the assumptions of normality and equal variances, ANOVA (followed by Tukey's HSD post-hoc test) or Student's *t*-test were implemented. In case of non-parametric data, Kruskal-Wallis followed by Dunn's post-hoc, or Wilcoxon test were employed.

When observations resulted extreme outliers, robust statistical methods such as one-way ANOVA for trimmed means or Yuen t-test were used (see details in Supplementary Information). In all cases, effect size was estimated accordingly, and confidence levels >95 % ($\alpha = 0.05$) were stablished in all statistical analyses.

3. Results

3.1. Climatic data and physicochemical properties of soils

No significant differences were detected between Sierra Nevada asymptomatic (NSH) and decline stands (NSD) for average temperature and annual rainfall; neither in the long term (40 years) nor in the short term (since 2000) (Table S1; Fig. S2A). The drought temporal series (SPEI-06) showed no significant differences among the study sites (Table S4). Several acute drought events of different intensity and severity among sites were identified (Fig. S2B), although the last severe drought episode (SPEI < −1.28) recorded in our study sites occurred in 2012. On the other hand, most of the edaphic properties differed among the sites under study (Table S5). The content of assimilable potassium (K) was the only parameter that varied between NSH and NSD soils, being significantly higher in the latter case.

3.2. General characteristics of deep sequencing data

A total of 5,720,859 (fungal) and 6,417,145 (bacterial) raw reads were retrieved from the Illumina platform, which resulted in 4,854,821 fungal and 2,302,311 bacterial high-quality sequences after all the trimming steps. Four samples had to be removed from the bacterial dataset due to the low number of sequences that passed the trimming process (< 2406 sequences). Eventually, 1064 and 690 fungal ASVs (rhizosphere soil and root endosphere, respectively), and 3403 (rhizosphere) and 1199 (root endosphere) bacterial ASVs were recorded (Table 1).

3.3. Describing the differences in the structure of root microbial populations

Statistical tests were only applied to compare samples corresponding to symptomatic versus asymptomatic trees located in Sierra Nevada, the only experimental site where both decline-affected and unaffected Scots pines were found. Comparisons between geographical units could bring to light differences due to abiotic and environmental factors (Philippot et al., 2013).

Fungal communities inhabiting the root endosphere of symptomless trees were significantly richer and more diverse than that associated to decline-affected trees. Similar pattern was observed for rhizosphere bacterial populations (Table 1). Both rhizosphere fungal and bacterial

Table 1
Bacterial and fungal alpha diversity indices calculated for rhizosphere soil and root endosphere samples obtained from Sierra de Almijara, Sierra de Baza and Sierra Nevada. Mean values of each group of samples ± standard deviation are shown. Asterisks indicate statistical significant differences in each index between symptomatic and asymptomatic trees located at Sierra Nevada (Student's *t*-test and two sample Yuen *t*-test, *p*-values <0.05). For those significant comparisons, the size of the effect is indicated (Cohen's d or Yuen's ξ).

	Area	Compartment	Status[a]	Observed ASVs		Shannon		InvSimpson[b]	Pielou	
Bacteria	Sierra de Almijara	Rhizosphere	Asymp.	593.58 ± 56.96		5.77 ± 0.16		132.78 ± 33.32	0.90 ± 0.02	
		Endosphere	Asymp.	144.00 ± 31.52		4.07 ± 0.28		31.75 ± 15.20	0.82 ± 0.04	
	Sierra de Baza	Rhizosphere	Symp.	612.42 ± 74.46		5.79 ± 0.26		167.80 ± 59.30	0.90 ± 0.03	
		Endosphere	Symp.	101.20 ± 43.06		2.88 ± 1.44		14.77 ± 12.33	0.61 ± 0.30	
	Sierra Nevada	Rhizosphere	Symp.	705.25 ± 60.12		5.87 ± 0.13*	d = 1.05	136.20 ± 27.96	0.90 ± 0.01*	d = 1.31
			Asymp.	685.42 ± 95.21		5.69 ± 0.21*		116.15 ± 30.37	0.87 ± 0.02*	
		Endosphere	Symp.	101.92 ± 83.89		1.09 ± 1.36		3.39 ± 5.24	0.22 ± 0.24	
			Asymp.	68.00 ± 59.57		0.61 ± 1.01		1.71 ± 2.03	0.13 ± 0.18	
Fungi	Sierra de Almijara	Rhizosphere	Asymp.	139.58 ± 18.81		3.27 ± 0.4		13.58 ± 6.17	0.66 ± 0.07	
		Endosphere	Asymp.	58.75 ± 16.90		2.31 ± 0.64		6.42 ± 3.59	0.57 ± 0.13	
	Sierra de Baza	Rhizosphere	Symp.	125.67 ± 19.00		3.24 ± 0.37		14.23 ± 10.38	0.67 ± 0.07	
		Endosphere	Symp.	45.33 ± 15.73		2.14 ± 0.52		5.90 ± 2.13	0.56 ± 0.11	
	Sierra Nevada	Rhizosphere	Symp.	139.75 ± 36.81		3.24 ± 0.85		17.02 ± 11.05	0.65 ± 0.15	
			Asymp.	130.50 ± 20.31		3.20 ± 0.61		12.95 ± 6.58	0.66 ± 0.12	
		Endosphere	Sympt.	53.50 ± 11.55*	ξ = 1.06	2.34 ± 0.41*	ξ = 1.06	6.55 ± 3.36	0.59 ± 0.10*	ξ = −0.85
			Asymp.	41.00 ± 12.06*		1.88 ± 0.46*		4.60 ± 1.96	0.51 ± 0.10*	

[a] Asymp., *Asyntomatic trees*; Symp, *Symptomatic trees.*
[b] InvSimpson, *Inverse of Simpson.*

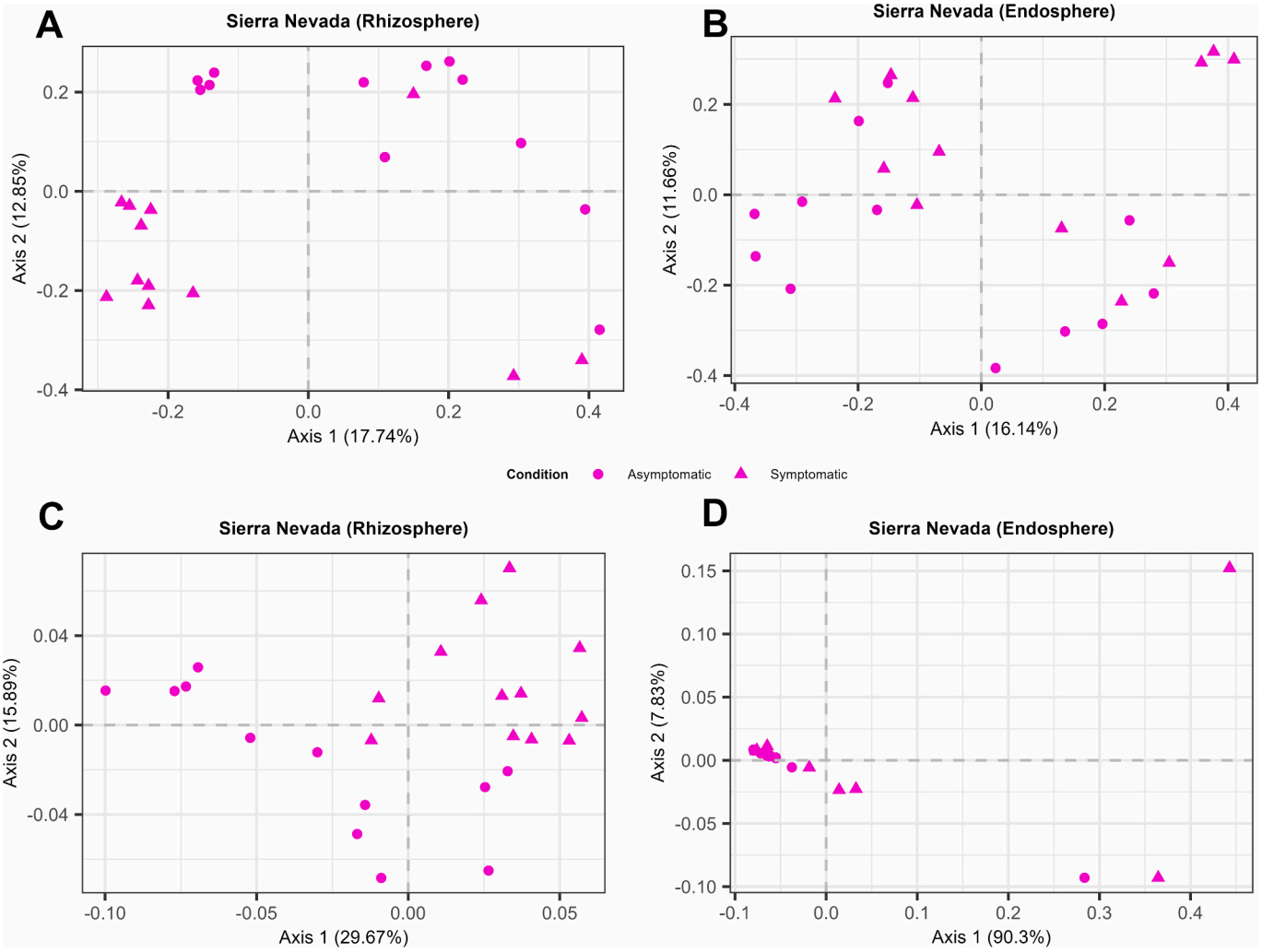

Fig. 1. Principal Coordinate Analysis (PCoA) of rhizosphere (A) and root endosphere (B) fungal communities, and rhizosphere (C) and bacterial communities inhabiting the root endosphere (D) of unaffected and decline symptoms-expressing *Pinus sylvestris* trees located at Sierra Nevada National Park. PCoA computed for fungal communities are based on Bray-Curtis dissimilarities, while Weighted UniFrac distances among bacterial communities were used.

communities of pine trees located in Sierra de Almijara grouped together and separatedly from samples of Sierra de Baza and Sierra Nevada across axis 1 and axis 2 of the PCoA, respectively (Fig. S3A and C). Considering just Sierra Nevada, rhizosphere samples of decline-affected trees clearly separated from samples of asymptomatic pines, both for fungi and bacteria (Fig. 1A and C). PERMANOVA confirmed that the structure of these microbial communities was significantly different from each other (Table 2). Nevertheless, the magnitude of these differences was subtle for fungal and bacterial communities (fungi: $\omega^2 = 0.069$; bacteria: $\omega^2 = 0.139$; Table 2). Microbial populations of the root endosphere did not follow the same pattern. While bacterial communities of decline-affected and asymptomatic trees located at Sierra Nevada did not show differences (PERMANOVA, $F = 0.93$, $p = 0.284$; Fig. 1D), significant albeit small differences were observed in the case of the mycobiome (Table 2; Fig. 1B).

3.4. Uncovering changes in the taxonomical composition of the root microbiota associated with pine forest decline

Rhizosphere mycobiome was dominated by *Basidiomycota* and *Ascomycota*, which accounted for >90 % of the total sequences in all sites under study (Fig. S4A). Remarkably, very minor differences were found when comparing the taxonomic profiles of decline-affected and unaffected trees located at Sierra Nevada (Table S6); only the phylum *Glomeromycota* resulted differentially abundant. Regarding the root endosphere, phyla *Ascomycota*, *Basidiomycota* and *Mucoromycota* were identified (Fig. S4B), but no significant differences were found in this case (Table S6).

Concerning the bacteriome, *Proteobacteria*, *Actinobacteria*, *Acidobacteria* and *Verrucomicrobia* accounted for >79 % of the total sequences retrieved from the rhizosphere dataset (Fig. S4C). Interestingly, sequences corresponding to Archaea were not detected. Among the main phyla, *Actinobacteria, Acidobacteria, Candidate division WPS-1* and *Planctomycetes* were significantly more represented in the rhizosphere of asymptomatic trees (Table S6), whilst only *Proteobacteria* was statistically more abundant in the rhizosphere of decline-affected individuals in Sierra Nevada (ANCOM-BC, $p < 2 \cdot 10^{-4}$). The composition of the root endosphere bacteriome depended on the geographic unit under study. Pines located at Sierra de Almijara were mainly enriched in phyla *Actinobacteria* and *Proteobacteria* (circa 90 % of the total sequences, see Fig. S4D), and trees located at Sierra de Baza and Sierra Nevada were also abundant in *Tenericutes*. No significant differences were found in the abundance of any of the bacterial phyla between symptoms-expressing and asymptomatic trees of Sierra Nevada (Table S6).

Going into deeper taxonomic level, fungal genera *Tricholoma*, *Hygrophorus*, *Inocybe, Clavulina, Hyaloscypha* and *Amphinema* were the most abundant taxa present in the rhizosphere. Nevertheless, their abundance depended on the mountainous area under study. Among the genera enriched in the rhizosphere of asymptomatic trees compared to that of decline-affected pines located in Sierra Nevada (ANCOM-BC; log-fold change, lfc < −1.5, $p < 0.05$), *Tylospora*, *Penicillium* and *Cladophialophora* accounted for >1.6 % of the total sequences (Fig. 2A). On the other hand, *Tomentella*, *Archaeorhizomyces* and *Pleomonodictys* were significantly more abundant in the rhizosphere soil of symptomatic trees (Fig. 2A). Concerning the root endosphere, genus *Pleomonodictys* was noticeably more abundant in decline-affected trees than in asymptomatic individuals, and it accounted for >4.5 % of the total sequences retrieved from this plant compartment (Fig. 2B).

With regard to the bacteriome, *Bradyrhizobium*, *Mycobacterium* and acidobacterial Gp6, Gp3 and Gp4 were the most abundant classified genera in the rhizosphere of trees located at all the studied sites (Table S7). It should be mentioned that the relative abundance of most of the differentially abundant genera was quite low (< 0.31 %, Table S6) with the exception of *Gp3*, which was subtly but significantly more abundant in the rhizosphere of symptomless trees (ANCOM-BC, lfc = −0.45, $p = 0.005$; Table S6). Regarding the root endosphere only 12 classified genera resulted significantly different in terms of abundance when comparing both types of trees, although both relative abundances and size of the differences were subtle (Fig. 2D; Table S6).

3.5. Deciphering the soil physicochemical parameters that shaped rhizosphere microbial communities

Among the edaphic parameters governing rhizosphere microbial communities, field capacity, clay percentage, soil pH, and bicarbonate content were key to explain differences found in the structure of the mycobiomes inhabiting the rhizosphere of pine trees located at all the sites under study (Fig. S5 A; Table S8). In contrast, none of the edaphic parameters under study were relevant to shape the fungal communities corresponding to trees located at Sierra Nevada (Table S8). On the other hand, content of assimilabe K and clay, and field capacity were determining factors explaining the structure of rhizosphere bacterial communities (envfit, $R^2 > 0.32$, $p = 0.001$; Fig. S5 B) when the three geographical units were considered. Notwithstanding, the content of assimilable K and the carbon-nitrogen ratio (C:N) were the best predictors of the rhizosphere bacteriome in Sierra Nevada (Table S8; Fig. S5C).

3.6. Root microbiota of decline-affected and asymptomatic pines assembles differently

All microbial associative networks calculated for Sierra Nevada did fit well with the power-law model ($R^2 > 0.86$), except for that inferred for the root endosphere of asymptomatic trees (R^2 of power law = 0.4), suggesting that the latter was not a scale-free network (Table 3). Co-occurrence network analyses demonstrated that members of microbial communities interacted in a different way in the rhizosphere depending on the trees' health status. The network corresponding to asymptomatic trees was more complex than that of decline-affected trees, as demonstrated by the higher values of average degree (avgK), average clustering coefficient (avgCC), number of nodes and links (Table 3). On the other hand, the network related to microbial communities inhabiting the rhizosphere of symptomatic pines showed higher levels of intramodular connections (Fig. 3B), which was endorsed with a significantly higher Centralization of stress centrality (Cs) value (Table 3). Microorganisms associated to decline-affected trees formed a higher compartimentalized network (significantly higher values of Geodesic Distance (GD) and number of modules) than that of unaffected pines (Table 3).

Table 2
Beta diversity of microbial communities dwelling in the rhizosphere soil and root endosphere of decline-affected and asymptomatic *P. sylvetris* trees located at Sierra Nevada. The model to be tested for PERMANOVA and PERMDISP2 analyses was *response variable* ~ *Condition*, being *Condition* the expression of decline symptoms (symptomatic or asymptomatic).

		PERMANOVA				PERMDISP2	
		R^2	F	*p*- value	Eff. size[a]	F	*p*- value
Bacteria	Rhizosphere	0.181	4.863	10^{-4}	0.139	6.858	0.02
	Endosphere	0.042	0.925	0.284	–	1.045	0.256
Fungi	Rhizosphere	0.112	2.786	$2{\cdot}10^{-4}$	0.069	0.880	0.388
	Endosphere	0.075	1.773	0.013	0.031	0.047	0.825

[a] Eff. Size, *Effect size.* Partial Omega Square values are shown.

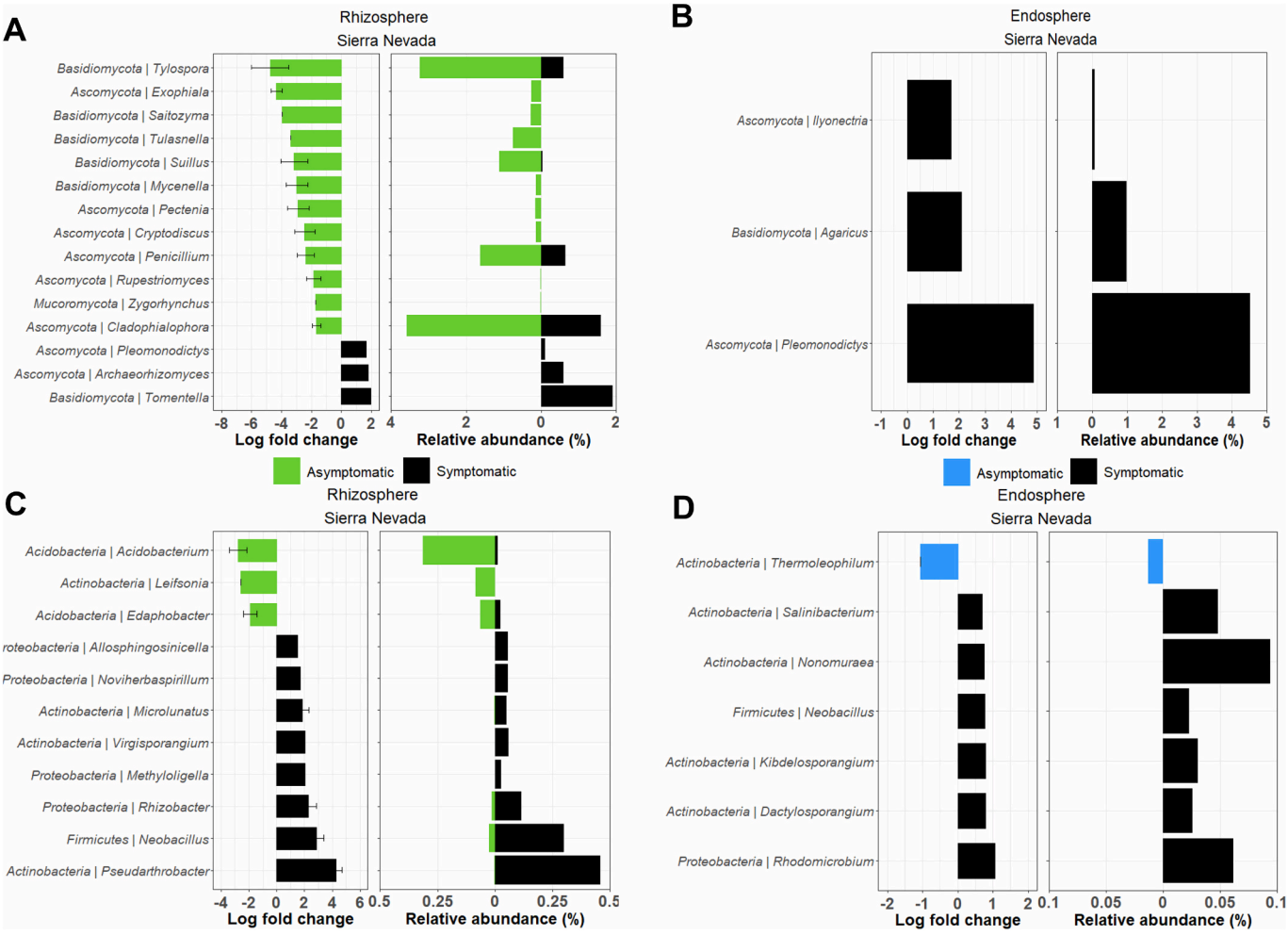

Fig. 2. Differential abundance (log fold change, lfc, calculated by ANCOM) and mean relative abundance for rhizosphere (A) and root endosphere fungal (B) and bacterial members dwelling in the rhizosphere (C) and root endosphere (D) of *Pinus sylvestris* trees located at Sierra Nevada. Just those genera with an associated lfc < -1.5 or lfc > 1.5 are showed, with the exception of root endosphere bacterial genera. Bars indicate the standard error of lfc values.

Table 3
Main topological properties of co-occurrence networks calculated for symptomatic and asymptomatic *P. sylvestris* trees located at Sierra Nevada. Asterisks denote significant differences in the corresponding parameter between both types of trees (Student's t-test, $p < 0.05$).

	Rhizosphere		Root endosphere	
	Symptomatic	Asymptomatic	Symptomatic	Asymptomatic
R^2 of power-law	0.95	0.931	0.857	0.401
Nodes	262	278	103	93
Links	280	321	136	172
Positive links (%)	30.36	29.91	25.74	5.23
Average degree (avgK)	2.137	2.309	2.641	3.699
Average clustering coefficient (avgCC)	0.014*	0.036*	0.103*	0.124*
Geodesic distance (GD)	6.899*	6.597*	5.606*	4.774*
Centratization of stress centrality (Cs)	0.748*	0.545*	0.477*	1.076*
Modularity	0.815	0.822	0.713*	0.638*
Modules	50	37	10	6

The microbiota inhabiting the root endosphere of diseased trees was assembled in a significantly higher modularized and less connected network than that of symptomless pines (Fig. 3D; Table 3). It is worth mentioning that the ASV00002 (genus '*Candidatus* Phytoplasma') was a member of the network corresponding to decline-affected pines, while it was not present in the network of unaffected trees.

Regarding the keystone hubs of co-occurrence networks computed for rhizosphere microbial communities, the connectors and module hubs resulted specific for each network type (Table S9). The same trend was observed for the networks corresponding to endosphere populations: none the connectors or module hubs of the network calculated for symptomatic network was found in that of unaffected trees, and *vice-versa* (Table S9).

3.7. *'Candidatus Phytoplasma pini' dominates the root endosphere of P. sylvestris trees in Sierra Nevada*

As shown in Fig.S6, some rarefaction curves calculated for the root

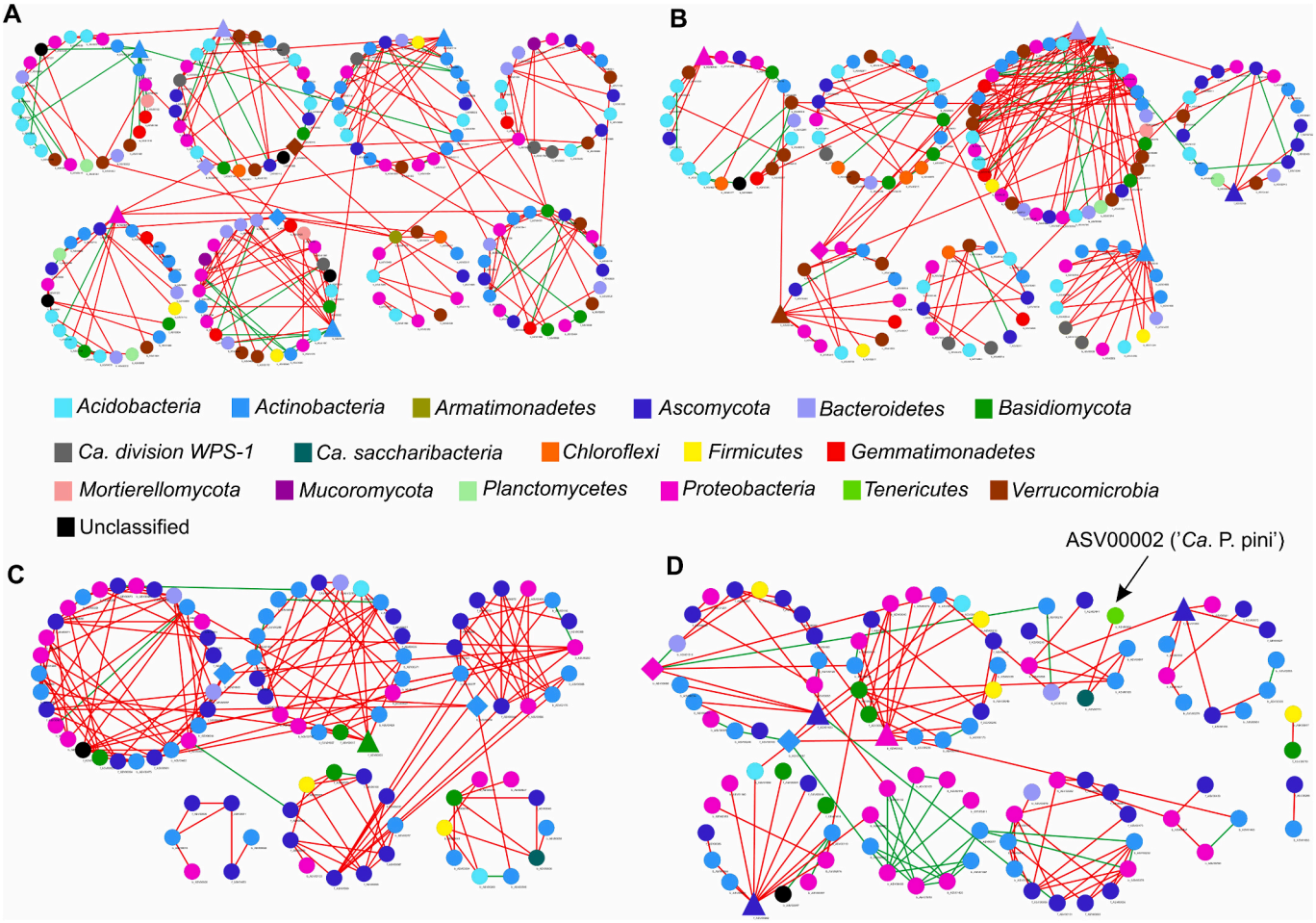

Fig. 3. Co-occurrence networks calculated for microbial populations inhabiting the rhizosphere of asymptomatic (A) and decline-affected (B) *Pinus sylvestris* trees, and root endosphere of unaffected (C) and symptomatic (D) pine trees located at Sierra Nevada. Triangle-shaped and diamond-shaped nodes represent module hubs and connector ASV, respectively. Red lines indicate positive links while those in red represent negative links.

endosphere of asymptomatic and decline-affected trees located at Sierra de Baza and Sierra Nevada reached the asymptote with a low number of ASVs. Pielou's evenness index did not exceed values of 0.22 (Table 1), demonstrating a great dominance at ASV level in the root endosphere of both types of trees. In line with alpha diversity, no statistical differences were recorded when the structure of the bacterial communities dwelling inside the root of symptomatic and unaffected trees of Sierra Nevada were compared (Table 2; Fig. 1D).

It is worth mentioning that the root endosphere of both types of trees were overwhelmingly dominated by only one ASV (ASV00002), belonging to the genus *Acholeplasma* according to the RDP database. The sequence of this ASV was also confronted with other databases (NCBI rRNA, SILVA SSU and EzBioCloud), and all of them classified it within the genus '*Candidatus* Phytoplasma' (phylum *Tenericutes*). This ASV accounted for 99.5 % of the total bacterial sequences retrieved from the root endosphere of some trees (Fig. 4A and B). However, no significant differences in the abundance of this ASV were found between decline-affected and asymptomatic pine trees located in Sierra Nevada. The root endosphere community of diseased trees in Sierra de Baza harboured >20 % of ASV00002 sequences, while a negligible number of sequences of this ASV was detected in Sierra de Almijara (Table S7).

Finally, six (asymptomatic) and 15 (decline-affected) clones from root endosphere samples of pines from Sierra Nevada were obtained. DNA inserts showed 99.7–99.9 % identity to the *16S rRNA* gene of '*Candidatus* Phytoplasma pini'. The phylogenetic tree (Fig. S7) showed that all cloned 16S rDNA sequences clustered together with '*Ca. P. pini* Pin127^{T}', confirming that all of cloned sequences belong to the species '*Candidatus* Phytoplasma pini'.

3.8. Unveiling the titer of 'Candidatus Phytoplasma pini' in the root endosphere of decline-affected and unaffected trees

No amplification was achieved at any of the temperatures tested when samples from the root endosphere of pine trees were used as template with the probe proposed by Christensen et al. (2004) for the generic detection of phytoplasmas.

With the probe Pr-CaPpini, phytoplasma-free verified samples and plant samples infected with '*Candidatus* Phytoplasma solani' (see Table S2), no amplification or Ct values higher than 28 and with signal intensity close to the threshold line were registered. On the contrary, both the standard curves and root endosphere samples amplified well with the probe Pr-CaPpini, recording Ct values ranging from 11 to 24. No qPCR inhibition phenomena were detected for any of the samples. Thereafter, phytoplasma titer determination was carried out with the probe Pr-CaPpini here designed.

Due to the very low DNA concentrations, eight and nine samples corresponding to asymptomatic and decline-affected pines, respectively, were considered for phytoplasma titration. Diseased trees showed more than four-fold higher '*Ca. P. pini*' titer than those registered for asymptomatic pines (Fig. 4C). Interestingly, this difference was statistically significant (Wilcoxon's test, $W = 13$, $p = 0.027$) and with a large effect size (Wilcoxon's $r = 0.537$).

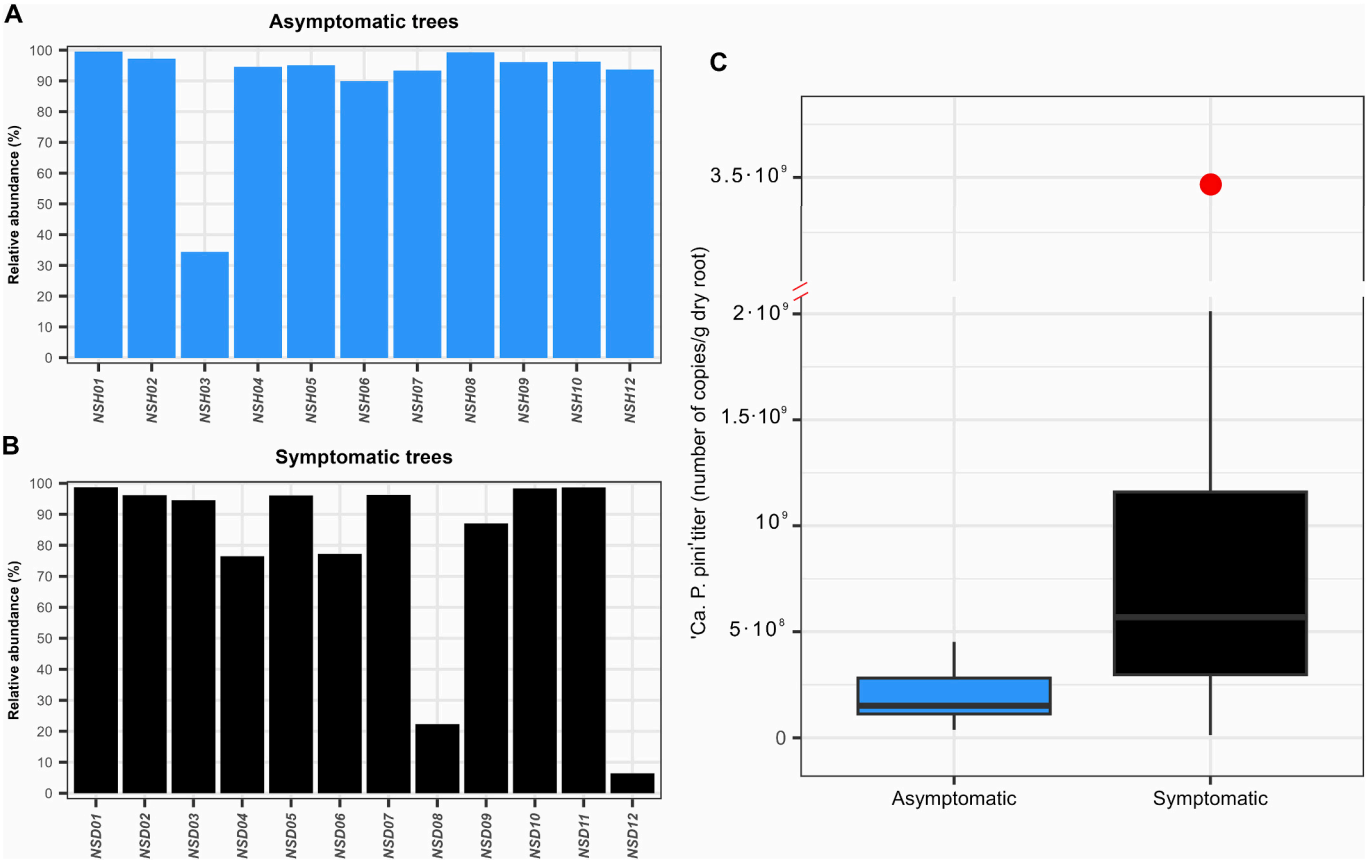

Fig. 4. Relative abundance of ASV0002 ('*Ca. P. pini*') in the rhizosphere of each asymptomatic (A) and symptomatic (B) *Pinus sylvestris* tree under study located in Sierra Nevada, and titers of '*Ca.* Phytoplasma pini' in decline-affected and unaffected trees ($N = 9$, $N = 8$, respectively). Titers of the phytopathogenic bacteria were measured by qPCR with the probe Pr-CaPpini.

4. Discussion

Forest decline is a disorder whose multifactorial nature makes it a difficult phenomenom to study and predict. Most of the studies have focused on the aerial part of decline-affected pines. In contrast, the potential role of the root microbiota in the decline process has been seldom investigated.

Our first hypothesis was partly met by the results obtained. Host trees' health status is a driving force of the differences observed in terms of alpha and beta diversity of root microbial communities, at least to some extent (Table 2). This suggests that other factors not considered in this study may also affect the structure of the root associated microbiota (rhizosphere and root endosphere). Contrary to what is commonly assumed for forest decline processes, drought episodes would not have been crucial factors for the pine decline scenario here reported, as supported by the absence of significant climatic differences between NSD and NSH sites.

Several minor genera, for which some species displaying plant growth promotion potential have been previously described, were more abundant in the rhizosphere of decline-affected than in asymptomatic pines located at Sierra Nevada. This was the case of *Neobacillus* (Hernández-Pacheco et al., 2021), *Dactylosporangium* (Kim et al., 2011) or *Kibdelosporangium* (Qin et al., 2015). Concerning the mycobiome, ECM fungi commonly associated with Scots pines (namely, genera *Tomentella*, *Tylospora* and *Suillus*) (Rudawska et al., 2018) were also differentially enriched in the rhizosphere of symptomatic or asymptomatic trees, depending on the genera. Although PGPM are commonly associated with healthy hosts, decline-affected trees may have deployed *cry-for-help* strategy (Rolfe et al., 2019) selectively recruiting or regulating the abundance of specific beneficial microorganisms to overcome the stress associated to the decline process. Nevertheless, it is difficult to infer the effect of the observed shifts in microbial abundance since most of the differentially registered bacterial genera were not very abundant, and certain genera could include both beneficial and pathogen members.

Pathogenic fungal genera affecting pine conifer species were also detected: *Cadophora* (previously identified as decline-causing fungal genus, Chen et al., 2022), *Gibberella* (to which the pathogen *G. circinata* belongs) *Heterobasidion* (including the pathogen *H. annosum*) and *Mycosphaerella,* which includes the pathogenic species *M. pini.* Since our experimental approach does not allow the identification of ASVs at the species level, actual presence of phytopathogenic fungal species can neither be confirmed nor ruled out. Thus, further research is needed to identify these fungal ASVs and unveil their role in pine decline events.

The balance of a microbial community does not only depend on its composition and structure, but also on the interactions among its members. It is generally assumed that complex and compact co-occurrence networks benefit plant hosts (Tao et al., 2018) and are positively correlated to lower incidence of phytopathogens in comparison to simpler networks (Yang et al., 2017; Fernández-González et al., 2020). Moreover, networks with tight arrangement (low values of GD and M) restrict the entry of invaders able to alter it (Cardinale et al., 2015), so they are considered to be more resistant to stresses. This is the scenario observed for the networks corresponding to asymptomatic trees, for both rhizosphere and root endosphere compartments. It is worth mentioning that the association network of the root endosphere (decline-affected trees) included one module in which the ASV00002 ('*Candidatus* Phytoplasma') was present, unlike the network corresponding to healthy trees. Our findings are thus in line with those reported by Fernández-González and co-workers (2020), who detected an

increase in modularity and GD values in the network of *Olea europaea* (susceptible cultivar Picual) plantlets infected by the pathogen *Verticillium dahliae*, which was also identified in one module of the network. Altogether, alterations in terms of microbial associations could be partly responsible of the decline symptomatology observed in the Scots pines located at Sierra Nevada National Park.

Differences observed in the root microbiota could be cause or consequence of the pine decline phenomenon. The question "which came first, the shifts in root microbial communities or the pine decline phenomenon?" cannot be answered at the moment, however, our results provide the first approach on the potential connection between the pine root microbiota and decline process. Moreover, our findings highlights that approaches intended to tackle the pine decline phenomena should not be based just on environmental and silvicultural factors, but they must also take into account root associated microbial communities.

Root endospheres, including that of woody plants, are commonly dominated by few bacterial taxa (Liu et al., 2017). It has been previously reported that just one OTU (Operational Taxonomic Unit) related to *Pseudomonas* accounted for up to 34 % of the total bacterial sequences retrieved from the root endosphere of *Populus deltoides* (Gottel et al., 2011), and the same was observed for genera *Actinophytocola* (22 %) and *Pseudomonas* (22–32 %) in the root endosphere of *Olea europea* and banana plants, respectively (Fernández-González et al., 2019; Gómez-Lama Cabanás et al., 2021). Intriguingly, and to the best of our knowledge, the high level of dominance of the ASV00002 ('*Candidatus* Phytoplasma', with a mean relative abundance higher than 79 %) has never been reported before. Members of '*Ca. P. pini*' displaced other bacteria inside the root of the Scots pines causing a dysbiosis in the host. Plant dysbioses entail a disruption of the holobiont homeostasis and could lead to the loss of essential functions linked to plant protection, nutrition or reproduction (Arnault et al., 2023). In addition, microbial diversity and evenness (two components that are a good barrier for microbial invaders (Berg et al., 2017) were drastically reduced in the root endosphere of both types of trees in Sierra Nevada. The conspicuous dominance of a specific microorganism (i.e., ASV00002) can thus make host pines more prone to the attack by invaders, since the control of pathogens, which is mostly maintained by competition between microorganisms, may be drastically impaired. Hence, *P. sylvestris* trees located at Sierra Nevada are not only dominated by a worrying pathogen but could also be threatened by outbreaks of oportunistic microorganisms or other stresses (Manion, 1991).

The presence of the phytopathogen in *P. sylvestris*, *P. halepensis* and *P. tabuliformis* trees that did not show phytoplasma-related symptoms has been erlier reported in Spain, Germany and Poland (Schneider et al., 2005; Kamińska et al., 2011; Morcillo et al., 2019). Currently, there is no consensus on why the phytoplasma prevails in non-symptomatic pine trees. While Stone and Putnam (2004) proposed that asymptomatic host pines could be tolerant to this pathogen, it is already known that symptoms can develop from seven days to 24 months after the inoculation of the pathogen by the vector (Hogenhout et al., 2008). The present work is the first one measuring the pathogen biomass since the vast majority of available studies dealing with '*Ca. P. pini*' have focused on the detection and taxonomy of the pathogen (Schneider et al., 2005; Śliwa et al., 2008; Kamińska et al., 2011; Ježić et al., 2013; Valiunas et al., 2015; Morcillo et al., 2019; Valiunas et al., 2019). Garcia et al. (2021) detected shifts in ethylene, phytohormones and biomass levels in surgacane plants infected with different titers of the phytopathogen *Leifsonia xyli* subsp. *Xyli*. Thus, although we cannot rule out that the pathogen was dormant at the time of sampling in the roots of symptomless trees, the differences registered in the titer of the pathogen suggested that the development of symptoms may be a consequence of having reached a specific titer of the pathogen. Several phytopathogenic bacteria have developed *quorum sensing* mechanisms, detecting a specific cell-density which activates their intercellular comunication systems and induces disease in the host plant (Gutiérrez-Pacheco et al., 2019). *Quorum sensing* has not been described for phytoplasmas yet, so further research is needed to elucidate the involvement of phytoplasmal cell density on the fitness of their host plants. Instead of triggering the decline phenomenon, '*Candidatus* Phytoplasma pini' could have weakened host trees in such a way that secondary adverse factor would have caused the decline event observed in some of the trees, as previously reported by Oliva et al. (2016) in *P. sylvestris* stands. In this sense, neither edaphic properties nor climatic conditions varied between NSD and NSH sites, so they can be discarded as contributing factors.

Finally, we would like to stress that most of the studies addressing the presence of phytoplasmas in conifers are based on nested PCR (EPPO, 2018) or qPCR procedures using the probe designed by Christensen et al. (2004) that in this study failed in the detection of '*Candidatus* Phytoplasma pini'. Hence, the incidence of the phytopathogen might well have been underestimated in forest ecosystems worldwile. Therefore, it is plausible to think that the impact of this phytopathogen is much higher than so far estimated.

5. Conclusions

Pine decline is commonly attributed to multiple tree stressors such as drought, high tree density, and/or pests. However, very little is known about the involvement of the root microbiota or how the decline process affects it. Our results highlight that the microbiota associated to the roots should not be overlooked when studying pine decline events, since enrichment in some fungi and bacteria has been undoubtedly observed at the belowground level of decline-affected trees. On the other hand, we alert about the incidence of fungal taxa with phytopathogenic potential that should be further identified at the species level. Moreover, both symptomless and decline-affected pine trees seemed to undergo a striking dysbiosis caused by the pathogen '*Candidatus* Phytoplasma pini'. In spite of the larger titer of this phytopathogen in symptoms-expressing trees, confirmation that this obligate parasite is the unique causal agent of pine decline needs further research. Indeed, it may act just as a predisposing factor weakening the trees to make them highly susceptible to other a/biotic stressors. Regardless of the succession of facts, we recommend to update the '*Candidatus* Phytoplasma pini' detection approaches to specifically detected it and to avoid massive spread and control of the phytopathogen.

Supplementary data to this article can be found online at https://doi.org/10.1016/j.scitotenv.2024.171858.

CRediT authorship contribution statement

Ana V. Lasa: Writing – review & editing, Writing – original draft, Validation, Software, Methodology, Investigation, Formal analysis, Data curation, Conceptualization. **Antonio José Fernández-González:** Writing – review & editing, Methodology, Investigation, Conceptualization. **Pablo J. Villadas:** Writing – review & editing, Methodology. **Jesús Mercado-Blanco:** Writing – review & editing. **Antonio J. Pérez-Luque:** Writing – review & editing, Software, Methodology, Investigation, Formal analysis, Conceptualization. **Manuel Fernández-López:** Writing – review & editing, Visualization, Supervision, Project administration, Investigation, Funding acquisition, Conceptualization.

Declaration of Generative AI and AI-assisted technologies in the writing process

Authors declare that generative AI neither AI-assisted technologies were used in the writing process of this manuscript.

Declaration of competing interest

The authors declare no competing financial interest or personal relationships that could have influenced the work reported in this paper.

Data availability statement

The datasets generated during the current study are available in the National Center for Biotechnology Information Sequence Read Archive repository (NCBI SRA) under the BioProject ID PRJNA993625. Nearly complete *16S rRNA* sequences of '*Ca. P. pini*' clones were deposited at the GenBank database and the corresponding accession numbers are indicated in Table S3.

Acknowledgements

This work was supported by the MICINN through European Regional Development Fund [SUMHAL, LIFEWATCH-2019-09-CSIC-13, POPE 2014-2020]. AJPL is currently funded by MCIN/AEI/10.13039/501100011033 and by "European Union NextGenerationEU/PRTR" with a "Juan de la Cierva" fellowship programme (Grant JDC2022-050056-I). We want to thank Dr. J. Sabaté for helping us with his knowledge on phytoplasmas.

References

Abarenkov, K., Zirk, A., Piirmann, T., Pöhönen, R., Ivanov, F., et al., 2022. UNITE general FASTA release for eukaryotes. v7.2 (version 7.2).

Ali, E., Cramer, W., Carnicer, J., Georgopoulou, E., Hilmi, N.J.M., et al., 2022. Cross-chapter paper 4: Mediterranean region. In: Pörtner, H.O., Roberts, D.C., Tignor, M., Poloczanska, E.S., Mintenbeck, K., et al. (Eds.), Climate Change 2022: Impacts, Adaptation and Vulnerability. Contribution of Working Group II to the Sixth Assessment Report of the Intergovernmental Panel on Climate Change. Cambridge University Press, Cambridge and New York, pp. 2233–2272.

Allen, C.D., Macalady, A.K., Chenchouni, H., Bachelet, D., McDowell, N., Vennetier, M., et al., 2010. A global overview of drought and heat-induced tree mortality reveals emerging climate change risks for forests. For. Ecol. Manage. 259, 660–684. https://doi.org/10.1016/j.foreco.2009.09.001.

Arnault, G., Mony, C., Vanderkoornhuyse, P., 2023. Plant microbiota dysbiosis and the Anna Karenina principle. Trends Plant Sci. 28, 18–30. https://doi.org/10.1016/j.tplants.2022.08.012.

Berg, G., Körbel, M., Rybakova, D., Müller, H., Grosch, R., Smalla, K., 2017. Plant microbial diversity is suggested as the key to future biocontrol and health trends. FEMS Microbiol. Ecol. 93, fix050. https://doi.org/10.1093/femsec/fix050.

Bettenfeld, P., Fontaine, F., Trouvelot, S., Fernandez, O., Courty, P.E., 2020. Woody plant declines. what's wrong with the microbiome? Trends Plant Sci. 25, 381–394. https://doi.org/10.1016/j.tplants.2019.12.024.

Bokulich, N.A., Subramanian, S., Fait, J.J., Gevers, D., Gordon, J.I., et al., 2013. Quality-filtering vastly improves diversity stimates form Illumina amplicon sequencing. Nat. Methods 10, 54–59. https://doi.org/10.1038/nmeth.2276.

Callahan, B.J., McMurdie, P.J., Rosen, M.J., Han, A.W., Johnson, A.J.A., et al., 2016. DADA2: high-resolution simple inference from Illumina amplicon data. Nat. Methods 13, 581–583. https://doi.org/10.1038/nmeth.3869.

Calvão, T., Duarte, C.M., Pimentel, C.S., 2019. Climate and landscape patterns of pine forest decline after invasion by the pinewood nematode. For. Ecol. Manage. 433, 43–51. https://doi.org/10.1016/j.foreco.2018.10.039.

Cardinale, M., Grube, M., Erlacher, A., Quehenberger, J., Berg, G., 2015. Bacterial networks and co-occurrence relationships in the lettuce root microbiota. Environ. Microbiol. 17, 239–252. https://doi.org/10.1111/1462-2920.12686.

Carnicer, J., Coll, M., Ninyerola, M., Pons, X., Sánchez, G., et al., 2011. Widespread crown condition decline, food web disruption, and amplified tree mortality with increased climate change-type drought. Proc. Natl. Acad. Sci. U. S. A. 108, 1474–1478. https://doi.org/10.1073/pnas.1010070108.

Chen, Q., Bakhshi, M., Balci, Y., Broders, K.D., Cheewangkoon, R., et al., 2022. Genera of phytopathogenis fungi: GOPHY 4. Stud. Mycol. 101, 417–564. https://doi.org/10.3114/sim.2022.101.06.

Christensen, N.M., Nicolaisen, M., Hansen, M., Schulz, A., 2004. Distribution of phytoplasmas in infected plants as revealed by real-time PCR and bioimaging. Mol. Plant Microbe Interact. 17, 1175–1184. https://doi.org/10.1094/mpmi.2004.17.11.1175.

Cole, J.R., Wang, Q., Fish, J.A., Chai, B., McGarrell, D.M., et al., 2014. Ribosomal database project: data and tools for high throughput rRNA analysis. Nucleic Acids Res. 42, 633–642. https://doi.org/10.1093/nar/gkt1244.

Connor, S.E., Araújo, J., Boski, T., Gomez, A., Gomes, S.D., et al., 2021. Drought, fire and grazing precursors to large-scale pine forest decline. Divers. Distrib. 27, 1138–1151. https://doi.org/10.1111/ddi.13261.

Denman, S., Doonan, J., Ransom-Jones, E., Broberg, M., Plummer, S., et al., 2018. Microbiome and infectivity studies reveal complex polyspecies tree disease in acute oak decline. ISME J. 12, 386–399. https://doi.org/10.1038/ismej.2017.170.

EPPO, 2018. Diagnostics PM 7/133 (1) generic detection of phytoplasmas. Bull OEPP. 48, 414–424. https://doi.org/10.1111/epp.12541.

Fernández-González, A.J., Villadas, P.J., Gómez-Lama Cabanás, C., Valverde-Corredor, A., Belaj, A., et al., 2019. Defining the root endosphere and rhizosphere microbiomes from the world olive germplasm collection. Sci. Rep. 9, 20423. https://doi.org/10.1038/s41598-019-56977-9.

Fernández-González, A.J., Cardoni, M., Gómez-Lama Cabanás, C., Valverde-Corredor, A., Villadas, P.J., et al., 2020. Linking belowground microbial network changes to different tolerance level towards Verticillium wilt of olive. Microbiome 8, 11. https://doi.org/10.1186/s40168-020-0787-2.

Gallart, M., Adair, K.L., Love, J., Meason, D.F., Clinton, P.W., et al., 2018. Genotypic variation in *Pinus radiata* responses to nitrogen source are related to changes in the root microbiome. FEMS Microbiol. Ecol. 94, fiy071. https://doi.org/10.1093/femsec/fiy071.

Garcia, F.H.S., Daneluzzi, G.S., Mazzafera, P., de Almeida, M., Nyheim, Ø., et al., 2021. Ratoon stunting disease (*Leifsonia xyli* subsp. *xyli*) affects source-sink relationship in sugarcane by decreasing sugar partitioning to tillers. Physiol. Mol. Plant Pathol. 116, 101723 https://doi.org/10.1016/j.pmpp.2021.101723.

Gómez-Lama Cabanás, C., Fernández-González, A.J., Cardoni, M., Valverde-Corredor, A., López-Cepero, J., et al., 2021. The banana root endophytome: differences between mother plants and suckers and evaluation of selected bacteria to control *Fusarium oxysporum* f.sp. *cubense*. J. Fungi. 7, 194. https://doi.org/10.3390/jof7030194.

Gottel, N.R., Castro, H.F., Kerley, M., Yang, Z., Pelletier, D.A., et al., 2011. Distinct microbial communities within the endosphere and rhizosphere of *Populus deltoides* roots across contrasting soil types. Appl. Environ. Microbiol. 77, 5934–5944. https://doi.org/10.1128/2FAEM.05255-11.

Guo, Y., Lin, Q., Chen, L., Carballar-Lejarazú, R., Zhang, A., et al., 2020. Characterization of bacterial communities associated with the pinewood nematode insect vector *Monochamus alternatus* Hope and the host tree *Pinus massoniana*. BMC Genomics 21, 337. https://doi.org/10.1186/s12864-020-6718-6.

Gutiérrez-Pacheco, M.M., Bernal-Mercado, A.T., Vázquez-Armenta, F.J., Martínez-Tellez, M.A., González-Aguilar, G.A., et al., 2019. *Quorum sensing* interruption as a tool to control virulence of plant pathogenic bacteria. Physiol. Mol. Plant. Pathol. 106, 281–291. https://doi.org/10.1016/j.pmpp.2019.04.002.

Hernández-Pacheco, C., Orozco-Mosqueda, M.C., Flores, A., Valencia-Cantero, E., Santoyo, G., 2021. Tissue-specific diversity of bacterial endophytes in Mexican husk tomato plants (*Physalis ixocarpa* Brot. Ex Horm.), and screening for their multiple plant growth-promoting activities. Curr. Res. Microb. Sci. 2, 100028 https://doi.org/10.1016/j.crmicr.2021.100028.

Hogenhout, S.A., Oshima, K., Ammar, E.D., Kakizawa, S., Kingdom, H.N., et al., 2008. Phytoplasmas: bacteria that manipulate plants and insects. Mol. Plant Pathol. 9, 403–423. https://doi.org/10.1111/2Fj.1364-3703.2008.00472.x.

Ihrmark, K., Bödeker, I.T.M., Cruz-Martinez, K., Friberg, H., Kubartova, A., et al., 2012. New primers to amplify the fungal ITS2 region – evaluation by 454- sequencing of artificial and natural communities. FEMS Microbiol. Ecol. 82, 666–677. https://doi.org/10.1111/j.1574-6941.2012.01437.x.

Ježić, M., Poljak, I., Šafarić, B., Idžojtić, M., Ćurković-Perica, M., 2013. 'Candidatus Phytoplasma pini' in pine species in Croatia. J. Plant. Dis. Prot. 120, 160–163. https://doi.org/10.1007/BF03356469.

Kamińska, M., Berniak, J., Obdrzalek, J., 2011. New natural host plants of '*Candidatus* Phytoplasma pini' in Poland and the Czech Republic. Plant Pathol. 60, 1023–1029. https://doi.org/10.1111/j.1365-3059.2011.02480.x.

Kim, B.Y., Kshetrimayum, J.D., Goodfellow, M., 2011. Detection, selective isolation and characterisation of Dactylosporangium strains from diverse environmental samples. Syst. Appl. Microbiol. 34, 606–616. https://doi.org/10.1016/j.syapm.2011.03.008.

Kumar, S., Stecher, G., Li, M., Knyaz, C., Tamura, K., 2018. MEGA X: molecular evolutionary genetics analysis across computing platforms. Mol. Biol. Evol. 35, 1547–1549. https://doi.org/10.1093/molbev/msy096.

Lasa, A.V., Mašinova, T., Baldrian, P., Fernández-López, M., 2019. Bacteria from the endosphere and rhizosphere of *Quercus* spp. use mainly cell wall-associated enzymes to decompose organic matter. PloS One 14, e0214422. https://doi.org/10.1038/ismej.2007.97.

Lasa, A.V., Guevara, M.A., Villadas, P.J., Vélez, M.D., Fernández-González, A.J., et al., 2022. Correlating the above- and belowground genotype of *Pinus pinaster* trees and rhizosphere bacterial communities under drought conditions. Sci. Total Environ. 832, 155007 https://doi.org/10.1016/j.scitotenv.2022.155007.

Lin, H., Peddada, S.D., 2020. Analysis of compositions of microbiomes with bias correction. Nat. Commun. 11, 3514. https://doi.org/10.1038/s41467-020-17041-7.

Liu, H., Carvalhais, L.C., Crawford, M., Singh, E., Dennis, P.G., et al., 2017. Inner plant values: diversity, colonization and benefits from endophytic bacteria. Front. Microbiol. 8, 2552. https://doi.org/10.3389/fmicb.2017.02552.

Lundberg, D.S., Yourstone, S., Mieczkowski, P., Jones, C.D., Dangl, J.L., 2013. Practical innovations for high-throughput amplicon sequencing. Nat. Methods 10, 999–1002. https://doi.org/10.1038/nmeth.2634.

Manion, P.D., 1991. Tree Disease Concepts, second ed. Prentice Hall Inc., Upper Saddle River.

Marcone, C., Valiunas, D., Mondal, S., Sundararaj, R., 2021. On some significant phytoplasma diseases of forest trees: an update. Forests 12, 408. https://doi.org/10.3390/f12040408.

Martin, M., 2011. Cutadapt removes adapter sequences from high-throughput sequencing reads. EMBnet J. 17, 10–12. https://doi.org/10.14806/ej.17.1.200.

Martínez-Vilalta, J., Aguadé, D., Banqué, M., Barba, J., Curiel Yuste, J., et al., 2012. Iberian scots pine populations under climate change: some don't like it hot. Ecosistemas 21, 15–21. https://doi.org/10.7818/ECOS.2012.21-3.03.

McMurdie, P.J., Holmes, S., 2013. Phyloseq: an R package for reproducible interactive analysis and graphics of microbiome census data. PloS One 8, e61217. https://doi.org/10.1371/journal.pone.0061217.

McMurdie, P.J., Holmes, S., 2014. Waste not, want not: why rarefying microbiome data is inadmissible. PLoS Comput. Biol. 10, e1003531 https://doi.org/10.1371/journal.pcbi.1003531.

Morcillo, L., Gallego, D., González, E., Vilagrosa, A., 2019. Forest decline triggered by phloem parasitism-related biotic factors in Aleppo pine (*Pinus halepensis*). Forests 10, 608. https://doi.org/10.3390/f10080608.

Mühling, M., Woolven-Allen, J., Colin Murrel, J., Joint, I., 2008. Improved group-specific PCR primers for denaturing gradient gel electrophoresis analysis of the genetic diversity of complex microbial communities. ISME J. 2, 379–392.

Oksanen, J., Simpson, G., Blanchet, F., Kindt, R., Legendre, P., et al., 2022. Vegan: community ecology package v2.6-4 (version 2.6-4). https://CRAN.R-project.org/package=vegan.

Olesen, J.M., Bascompte, J., Dupont, Y.L., Jordano, P., 2017. The modularity of pollination networks. Proc. Natl. Acad. Sci. U. S. A. 104, 19891–19896. https://doi.org/10.1073/pnas.0706375104.

Oliva, J., Stenlid, J., Grönkvist-Wichmann, L., Wahlström, M., Drobyshev, I., et al., 2016. Pathogen-induced defoliation of *Pinus sylvestris* leads to tree decline and dead from secondary biotic factors. For. Ecol. Manage. 379, 273–280. https://doi.org/10.1016/j.foreco.2016.08.011.

Páscoa, P., Gouveia, C.M., Russo, A., Trigo, R.M., 2017. Drought trends in the Iberian Peninsula over the last 112 years. Adv. Meteorol. 2017, 4653126. https://doi.org/10.1155/2017/4653126.

Philippot, L., Raaijmakers, J.M., Lemanceau, P., van der Putten, W.H., 2013. Going back to the roots: the microbial ecology of the rhizosphere. Nat. Rev. Microbiol. 11, 789–799. https://doi.org/10.1038/nrmicro3109.

Proença, D.N., Francisco, R., Kublik, S., Schöler, A., Vestergaard, G., et al., 2017. The microbiome of endophytic, wood colonizing bacteria from pine trees as affected by pine wilt disease. Sci. Rep. 7, 4205. https://doi.org/10.1038/s41598-017-04141-6.

Qin, S., Feng, W.W., Xing, K., Bai, J.L., Yuan, B., et al., 2015. Complete genome sequence of *Kibdelosporangium phytohabitans* KLBMP 1111T, a plant growth promoting endophytic actinomycete isolated from oil-seed plant *Jatropha curcas* L. J. Biotechnol. 216, 129–130. https://doi.org/10.1016/j.jbiotec.2015.10.017.

R Core Team, 2022. R: A language and environment for statistical computing. https://www.R-project.org/.

Rolfe, S.A., Griffithss, J., Ton, J., 2019. Crying out for help with root exudates: adaptive mechanisms by which stressed plants assemble health-promoting soil microbiomes. Curr. Opin. Microbiol. 49, 73–82. https://doi.org/10.1016/j.mib.2019.10.003.

Rudawska, M., Wilgan, R., Janowski, D., Iwański, M., Leski, T., 2018. Shifts in taxonomical and functional structure of ectomycorrhizal fungal community of scots pine (*Pinus sylvestris* L.) underpinned by partner tree ageing. Pedobiologia 71, 20–30. https://doi.org/10.1016/j.pedobi.2018.08.003.

Sánchez-Salguero, R., Navarro-Cerrillo, R.M., Swetnam, T., Zavala, M.A., 2012. Is drought the main decline factor at the rear edge of Europe? The case of southern Iberian pine plantations. For. Ecol. Manage. 271, 158–169. https://doi.org/10.1016/j.foreco.2012.01.040.

Sasada, R., Weinstein, M., Prem, A., Jin, M., Bhasin, J., 2020. FIGARO: an efficient and objective tool for optimizing microbiome rRNA gene trimming parameters. J. Biomol. Tech. 31, S2. https://doi.org/10.1101/610394.

Schneider, B., Torres, E., Martín, M.P., Schröder, M., Behnke, H., et al., 2005. '*Candidatus* Phytoplasma pini', a novel taxon from *Pinus silvestris* and *Pinus halepensis*. Int. J. Syst. Evol. Microbiol. 55, 303–307. https://doi.org/10.1099/ijs.0.63285-0.

Shannon, P., Markiel, A., Ozier, O., Baliga, N.S., Wang, J.T., et al., 2003. Cytoscape: a software environment for integrated models of biomolecular interaction networks. Genome Res. 13, 2498–2504. https://doi.org/10.1101/gr.1239303.

Śliwa, H., Kaminska, M., Korszun, S., Adler, P., 2008. Detection of '*Candidatus* Phytoplasma pini' in *Pinus sylvestris* trees in Poland. J. Phytopathol. 156, 88–92. https://doi.org/10.1111/j.1439-0434.2007.01335.x.

Spinoni, J., Vogt, J.V., Naumann, G., Barbosa, P., Dosio, A., 2017. Will drought events become more frequent and severe in Europe? Int. J. Climatol. 38, 1718–1736. https://doi.org/10.1002/joc.5291.

Stone, J.K., Putnam, M.L., 2004. Pathology. Leaf and needle diseases. In: Burley, J., Evans, J., Youngquist, J.A. (Eds.), Encyclopedia of Forest Sciences. Elsevier Ltd., Oxford, pp. 777–785.

Takahashi, S., Tomita, J., Nishioka, K., Hisada, T., Nishijima, M., 2014. Development of a prokaryotic universal primer for simultaneous analysis of bacteria and archaea using next-generation sequencing. PloS One 9, 8. https://doi.org/10.1371/journal.pone.0105592.

Tao, J., Meng, D., Qin, C., Liu, X., Liang, Y., et al., 2018. Integrated network analysis reveals the importance of microbial interactions for maize growth. Appl. Microbiol. Biotechnol. 102, 3805–3818. https://doi.org/10.1007/s00253-018-8837-4.

Trujillo-Toro, J., Navarro-Cerrillo, R.M., 2019. Analysis of site-dependent *Pinus halepensis* mill. Defoliation caused by '*Candidatus* Phytoplasma pini' through shape selection in Landsat time series. Remote Sens. (Basel) 11, 1868. https://doi.org/10.3390/rs11161868.

Uroz, S., Buée, M., Deveau, A., Mieszkin, S., Martin, F., 2016. Ecology of the forest microbiome: highlights of temperate and boreal ecosystems. Soil Biol. Biochem. 103, 471–488. https://doi.org/10.1016/j.soilbio.2016.09.006.

Valiunas, D., Jomantiene, R., Ivanauskas, A., Urbonaite, I., Sneideris, D., et al., 2015. Molecular identification of Phytoplasmas infecting diseased pine trees in the UNESCO-protected Curonian spit of Lithuania. Forests 6, 2469–2483. https://doi.org/10.3390/f6072469.

Valiunas, D., Jomantiene, R., Ivanauskas, A., Sneideris, D., Zizyte-Eidetiene, M., et al., 2019. Rapid detection and identification of '*Candidatus* Phytoplasma pini'-related strains based on genomic markers present in *16S rRNA* and *tuf* genes. For. Pathol. 49, e12553 https://doi.org/10.1111/efp.12553.

Vicente-Serrano, S.M., Beguería, S., López-Moreno, J.I., 2010. A multiscalar drought index sensitive to global warming: the standardized precipitation evapotranspiration index. J. Climate 23, 1696–1718. https://doi.org/10.1175/2009JCLI2909.1.

Vicente-Serrano, S.M., Domínguez-Castro, F., Reig, F., Beguería, S., Tomas-Burguera, M., et al., 2022. A near real-time drought monitoring system for Spain using automatic weather station network. Atmos. Res. 271, 106095 https://doi.org/10.1016/j.atmosres.2022.106095.

Vidal-Macua, J.J., Ninyerola, M., Zabala, A., Domingo-Marimon, C., Pons, X., 2017. Factors affecting forest dynamics in the Iberian Peninsula from 1987 to 2012. The role of topography and drought. For. Ecol. 406, 290–306. https://doi.org/10.1016/j.foreco.2017.10.011.

White, T.J., Bruns, T.D., Lee, S.B., Taylor, J.W., 1990. Amplification and direct sequencing of fungal ribosomal RNA genes for phylogenetics. In: Innis, M.A., Gelfand, D.H., Sninsky, J.J., White, T.J. (Eds.), PCR Protocols: A Guide to Methods and Applications. Academics Press, San Diego, pp. 315–322.

Yang, H., Li, J., Xiao, Y., Gu, Y., Liu, H., et al., 2017. An integrated insight into the relationship between soil microbial community and tobacco bacterial wilt disease. Front. Microbiol. 8, 2179. https://doi.org/10.3389/fmicb.2017.02179.

Yoon, S.H., Ha, S.M., Kwon, S., Lim, J., Kim, Y., et al., 2014. Introducing EzBioCloud: a taxonomically united database of 16S rRNA and whole genome assemblies. Int. J. Syst. Evol. Microbiol. 67, 1613–1617. https://doi.org/10.1099/2Fijsem.0.001755.